Current Research in Food Science 5 (2022) 288–297

Contents lists available at ScienceDirect

Current Research in Food Science

journal homepage: www.sciencedirect.com/journal/current-research-in-food-science

Fabrication and characterization of core-shell gliadin/tremella polysaccharide nanoparticles for curcumin delivery: Encapsulation efficiency, physicochemical stability and bioaccessibility

Xiaomin Zhang [a], Zihao Wei [a,*], Xin Wang [a], Yuming Wang [a], Qingjuan Tang [a], Qingrong Huang [c], Changhu Xue [a,b]

[a] College of Food Science and Engineering, Ocean University of China, Qingdao, 266003, China
[b] Laboratory of Marine Drugs and Biological Products, Pilot National Laboratory for Marine Science and Technology (Qingdao), Qingdao, 266237, China
[c] Department of Food Science, Rutgers University, 65 Dudley Road, New Brunswick, NJ, 08901, United States

ARTICLE INFO

Keywords:
Gliadin
Tremella polysaccharide
Curcumin
Physicochemical stability
Bioaccessibility

ABSTRACT

The objectives of the present study were to synthesize gliadin/tremella polysaccharide nanoparticles (Gli/TP NPs) as well as curcumin-loaded gliadin/tremella polysaccharide nanoparticles (Cur-Gli/TP NPs) and evaluate the encapsulation efficiency (EE), physicochemical stability and bioaccessibility of Cur-Gli/TP NPs. The physicochemical properties of the nanoparticles depended on the mass ratio of Gli to TP and pH values. The characterization of the Gli/TP NPs indicated that the prepared nanoparticles were the most stable when the Gli/TP mass ratio was 1:1 and pH was at 4.0–7.0. Afterward, prepared Cur-Gli/TP NPs at different pH values were studied. Compared with the EE of Cur (58.2%) in Cur-Gli NPs at pH 5.0, the EE of Cur (90.6%) in Cur-Gli/TP NPs at pH 5.0 was increased by 32.4%. Besides, the Cur-Gli/TP NPs possessed excellent physical stability, photostability, thermal stability and re-dispersibility than Cur-Gli NPs. Furthermore, the bioaccessibility of Cur reached 83.5% after encapsulation of Cur into Gli/TP NPs after *in vitro* digestion, indicating that Cur-Gli/TP NPs could improve curcumin bioaccessibility significantly. In summary, this study demonstrates that the new food-grade Gli/TP NPs possess high encapsulation efficiency, excellent stability and prominent nutraceutical bioaccessibility. Meanwhile, it contributes to expanding the application of TP in food-grade delivery systems.

1. Introduction

Curcumin (Cur) is a natural dietary polyphenol extracted from turmeric roots and has aroused extensive attention for its potential health-benefiting biological activities such as anti-cancer, antioxidant, anti-inflammatory, antimicrobial and neuroprotective activities (Wei and Huang, 2019; Zhan et al., 2020). However, the application of Cur in food products is extremely limited due to its comprehensive roles of poor water solubility, photodegradation, thermal degradation, low absorption and instability under gastrointestinal conditions (Chen et al., 2021; Feng et al., 2020; Dhingra et al., 2021). Therefore, it is necessary to explore a suitable strategy to solve these problems hindering application of Cur in functional foods. During the past few years, protein-based nanoparticle as a delivery vehicle of bioactive components has attracted increasing scientific and industrial attention owing to its desirable properties such as excellent stability against UV light as well as high temperature and high encapsulation capacity. Moreover, bioactive ingredients-loaded protein nanoparticles exhibit higher stability as well as delayed-release behavior in simulated gastrointestinal digestion (Feng et al., 2020; Xin et al., 2020; Yuan et al., 2021; Zhan et al., 2020). In this background, encapsulating Cur in protein nanoparticles may be a promising mean to overcome the aforementioned defects of restricting the application of Cur and expand its applicability.

Gliadin (Gli), an alcohol-soluble protein extracted from wheat, has outstanding ability to form delivery systems to deliver hydrophobic bioactive ingredients due to its natural amphiphilicity and self-assembly capability (Peng et al., 2018; Su et al., 2021; Yang et al., 2021). Recent studies have shown that Gli can form food-grade nanoparticles (NPs) by anti-solvent method, and Gli NPs have ability to encapsulate sensitive functional ingredients. In addition, Gli NPs exhibit excellent mucoadhesive properties during gastrointestinal digestion and absorption, which is beneficial to increasing the bioaccessibility of embedded

* Corresponding author.
E-mail address: weizihao@ouc.edu.cn (Z. Wei).

https://doi.org/10.1016/j.crfs.2022.01.019
Received 13 December 2021; Received in revised form 19 January 2022; Accepted 23 January 2022
Available online 29 January 2022

bioactive compounds (Yang et al., 2018; Zheng et al., 2021). Therefore, Gli NPs as oral delivery vehicles of Cur have broad application prospects. However, NPs produced from Gli only still have limitations (e.g., easy aggregation, relatively low encapsulation efficiency) in encapsulating bioactive ingredients. Appealingly, the Gli NPs prepared by coating a layer of polysaccharide exhibited more excellent behavior in enhancing the stability and encapsulation efficiency of bioactive ingredients (Yang et al., 2018).

Tremella polysaccharide (TP) is a non-cytotoxic biological macromolecule extracted from tremella, possessing multiple biological functions (anti-oxidation, anti-inflammation, anti-aging, reducing blood lipids, immune regulation, etc.) (Ge et al., 2020; Wu et al., 2019; Xiao et al., 2021; Xu et al., 2020). In addition, TP has many excellent physicochemical properties such as film-forming, lubrication and water retention (Niu et al., 2021). These attractive physicochemical properties and the anionic properties endow TP with ability to form a delivery system by interacting with other biological macromolecules. For examples, NPs were produced by interaction between TP and chitosan, and these NPs could be employed as carriers to encapsulate nutraceuticals and improve their oral absorption efficiency (Wang et al., 2019). TP could be assembled with carboxymethyl cellulose (CMC) and nonionic surfactant-decyl polyglucoside (C_{10}APG) to form a novel pH/temperature responsive micelle-laden hydrogel, further applied to control the release of bioactive ingredients (Zhao and Li, 2020). However, the study on encapsulating and delivering hydrophobic bioactive ingredients with Gli/TP NPs to improve their stability and bioaccessibility has not been explored.

In this study, Gli/TP NPs were prepared by anti-solvent method under different Gli/TP mass ratios and pH values. Afterward, the properties of prepared nanoparticles were characterized. Considering that nanoparticle at different pH values may exhibit different structural and functional properties, it was intriguing to investigate the physicochemical stability of Cur-loaded Gli/TP NPs at different pH values. The particle size, polydispersity index (PdI) as well as zeta-potential of the nanoparticles and the encapsulation efficiency (EE) of Cur were measured. The physical stability, photostability, thermal stability and re-dispersibility of Cur-loaded Gli/TP NPs were investigated and compared with that of Cur-loaded Gli NPs (without TP). Finally, the bioaccessibility of Cur encapsulated in Gli/TP NPs (or without TP) was studied by *in vitro* digestion. The present work may provide a new route to develop novel delivery carrier of bioactive compounds. Meanwhile, it contributes to expanding the application of TP in food-grade delivery systems.

2. Materials and methods

2.1. Materials

Gliadin (Gli) from wheat was purchased from the Shanghai Macklin Biochemical Company (Shanghai, China). Curcumin (Cur, ≥95.0% purity) was obtained from the Shanghai Ryon Biological Technology CO. Ltd (Shanghai, China). Tremella was provided by Qingdao Marine Food Nutrition and Health Innovation Research Institute (Qingdao, China). Absolute ethanol (99.99%) was provided by Tianjin Fuyu Fine Chemical CO. Ltd (Tianjin, China). Pig bile salt was purchased from Gloden-clone Biological Technology Co. Ltd (Beijing, China). Pancreatin, pepsin and tris were purchased from Solarbio company (Beijing, China), Calcium chloride anhydrous was provided by Sinopharm Chemical Reagent Co. Ltd. All other chemicals are of analytical grade unless otherwise indicated.

2.2. Extraction of tremella polysaccharide (TP)

The dry tremella was soaked in deionized water at pH 7.6 to make it extremely expand. The condition of fat removal was to soak tremella in deionized water at 60 °C and pH 9.0–10.0 for 0.5 h. Then the tremella was removed from the lye solution and soaked in an acidic solution adjusted with citric acid to pH 6.0–6.5 for 20–40 min. TP was extracted by hydrothermal method with steps as follows (Wang et al., 2019): (1) the tremella was taken out from acidic solution and drained to obtain dry tremella; (2) the dry tremella was pulverized and put into a filter bag, where the TP was extracted in water bath adjusted to 100 °C for 4 h; (3) removing extracting solution and then adding water to precipitate. To decrease the viscosity of extracting solution, the protein in extracting solution was hydrolyzed with 1% neutral protease as well as 0.1% papain, and the reaction was kept at 50 °C in water bath for 3 h. After removing these enzymes, the mixture was filtered with diatomite to obtain crude polysaccharide.

2.3. Fabrication of core-shell Gli/TP NPs

2.3.1. Fabrication of nanoparticles with different Gli/TP mass ratios

The Gli/TP NPs were prepared by the anti-solvent method (Su et al., 2021). Briefly, 400 mg of Gli was dispersed in ethanol-water solution (10 mL, 70:30, v/v), followed by stirring (300 rpm, 1.5 h) to form stock solution. The resultant solution (40 mg/mL) was obtained by centrifugating the stock solution at 4000 rpm for 20 min to remove insoluble Gli. The Gli NPs (i.e., control sample) dispersion was formed by slowly adding 1 mL of Gli supernatant to 19 mL of deionized water and then stirring continuously (300 rpm) for 30 min. TP of different masses (200 mg, 400 mg and 800 mg) was dissolved in 200 mL of deionized water and then slowly added to Gli NPs solution of the same volume, followed by continuously stirring (300 rpm) for 30 min to form Gli/TP NPs with diverse Gli/TP mass ratios (2:1, 1:1, 1:2) (Yu et al., 2021). Samples prepared with different mass ratios of Gli to TP were named as Gli/TP NPs 2:1, Gli/TP NPs 1:1 and Gli/TP NPs 1:2, respectively. Control samples were termed as Gli NPs (Gli: gliadin, TP: tremella polysaccharide).

2.3.2. Fabrication of nanoparticles with different pH values

The preparation method of Gli supernatant (40 mg/mL) was the same as that in 2.3.1. 1 mL of Gli supernatant was injected into 19 mL of deionized water to prepare Gli NPs (2 mg/mL). According to the optimal mass ratio in section 2.3.1, TP aqueous solution was prepared. At room temperature, TP aqueous solution was dripped into the freshly prepared Gli NPs dispersion of the same volume to obtain Gli/TP NPs. The pH values of Gli/TP NPs solution after particle assembly were adjusted to 3.0, 4.0, 5.0, 6.0 and 7.0 using hydrochloric acid and sodium hydroxide solution (0.01 M) to form Gli/TP NPs with different pH values.

2.4. Particle size, polydispersity index (PdI) and zeta-potential measurements

Particle size, PdI and zeta-potential of Gli/TP NPs with different Gli/TP mass ratios and pH values were measured by Nano-ZS90 (Malvern Instruments, Worcestershire, UK) (Wu et al., 2020). Briefly, 1 mL of nanoparticle dispersion was placed in the measurement cell and then detected by Nano-ZS90. These samples were diluted to a suitable concentration with deionized water before determination to obtain the optimal instrument sensitivity (Wei et al., 2019a,b,c,d). Each sample was tested three times and test results were expressed as mean ± standard deviation.

2.5. Turbidity measurement

Turbidity is generally considered to be related to the size and number of nanoparticles. According to the method of Wu et al. (2020), the %T of Gli/TP NPs at different Gli/TP mass ratios and pH values was measured using a UV-2355 spectrophotometer (UNICO (Shanghai) Instrument CO. Ltd) at 426 nm (Wu et al., 2020). Then, the turbidity of these nanoparticles could be obtained by simply calculating 100-%T. All samples were measured at 25 °C and each sample was measured three times.

2.6. Preparation of Cur-loaded Gli/TP NPs

The Gli supernatant was prepared as described above. The mass ratios of Gli to Cur were 4:1, 2:1 and 1:1, respectively. Gli–Cur mixture solution was prepared by dissolving Cur (100 mg, 200 mg and 400 mg) into Gli supernatant under magnetic stirring, and then the acquired solution was centrifuged at 4000 rpm for 20 min to remove insoluble Cur. Prepared samples with different Gli/Cur mass ratios were named as Cur-Gli/TP NPs 4:1, Cur-Gli/TP NPs 2:1 and Cur-Gli/TP NPs 1:1, respectively. Control samples were termed as Cur-Gli NPs (Cur: curcumin).

The preparation method of Cur-Gli/TP NPs was as follows: briefly, 1 mL of Gli–Cur mixture solution with different Gli/Cur mass ratios was slowly dropped into 19 mL of deionized water (pH 5.0) to prepare Cur-Gli NPs. Then, the prepared TP aqueous solution (2 mg/mL) was slowly added to Cur-Gli NPs dispersion of the same volume under continuous stirring (300 rpm, 30 min). Finally, the Cur-Gli/TP NPs were adjusted to pH 4.0, 5.0 and 7.0 using 0.01 M HCl/NaOH under magnetic stirring to prepare the nanoparticles with different pH values. Cur-Gli NPs with different pH values were used as control samples.

2.7. Particle size, PdI and zeta-potential measurements

The method was the same as 2.4.

2.8. Determination of encapsulation efficiency

The encapsulation efficiency (EE) of the Cur-loaded nanoparticles was determined according to the method described in reference (Meng et al., 2021). Briefly, 1 mL of freshly prepared nanoparticle dispersion was centrifuged at 10,000 rpm at 4 °C for 30 min to acquire supernatant solution. The solution was diluted to a suitable concentration with 4.0 mL ethanol–water solution (95%, v/v). Then, the absorbance of the above solution was measured at 426 nm with a UV-2355 spectrophotometer. The content of Cur was calculated by using a suitable calibration curve: $y = 0.1563x - 0.0021$ ($R^2 = 0.9989$; y is the absorbance; x is Cur concentration). Then the EE of Cur was calculated as follows:

$$EE(\%) = \left(\frac{total\ Cur - free\ Cur}{total\ Cur}\right) \times 100\% \quad (1)$$

2.9. Physical stability analysis

At room temperature (25 °C), the physical stability of Cur-Gli/TP NPs and Cur-Gli NPs at pH 4.0, 5.0 and 7.0 was evaluated by static multiple gravity light scattering using a TurbiscanLAB (Formulaction, France). 10 mL of sample was slowly dropped into a cell. The instrument scanned the transmitted photons (T) and backscattered photons (BS) of the nanoparticles in each sample for 0.5 h and the measurement interval was 1 min. The resulting profile was reported as a function of transmittance (ΔT) and backscattering (ΔBS), which was expressed as the Turbiscan Stability Index (TSI) (Gagliardi et al., 2021; Voci et al., 2021).

2.10. UV light and thermal stability analyses

In order to analyze the photostability of Cur-Gli/TP NPs and Cur-Gli NPs at pH 4.0, 5.0 and 7.0, all samples were placed in transparent glass vials and exposed to UV light for 120 min. 1 mL of sample was taken at 30, 60, 90 and 120 min, respectively and then diluted 5 times with 95% ethanol–water solution to determine the content of residual Cur. Cur-Gli NPs at pH 4.0, 5.0 and 7.0 were used as control samples. The content of Cur was measured by a UV-2355 spectrophotometer (UNICO (Shanghai) Instrument CO. Ltd). The retention rate of Cur after UV treatment was evaluated based on the initial Cur concentration of the sample at 0 min (Yang et al., 2018).

In order to analyze the thermal stability of Cur-Gli/TP NPs and Cur-Gli NPs at pH 4.0, 5.0 and 7.0, all samples were placed in transparent glass vials and incubated in a thermostatic water bath at 40 °C and 60 °C for 30 min, respectively. Then they were quickly cooled to room temperature. Each sample was diluted 5 times with 95% ethanol–water solution to determine the concentration of residual Cur. Cur-Gli NPs at pH 4.0, 5.0 and 7.0 were used as control samples. The content of Cur was measured by a UV-2355 spectrophotometer (UNICO (Shanghai) Instrument CO. Ltd). The retention rate of Cur after thermal treatment was evaluated based on the initial Cur concentration of the sample at 0 min (Chen et al., 2021). The retention rate of Cur is calculated by the following formula:

$$Retention\ rate(\%) = \frac{mass\ of\ residual\ Cur}{total\ mass\ of\ Cur\ in\ initial\ nanoparticle} \times 100\% \quad (2)$$

2.11. Re-dispersibility

All freeze-dried Cur-Gli/TP NPs and Cur-Gli NPs at pH 4.0, 5.0 and 7.0 were dissolved in deionized water to a concentration of 1 mg/mL and then stirred at 300 rpm for 30 min to completely re-disperse. The dispersion results of each sample were then observed (Wu et al., 2020). The particle size and PdI of the re-dispersed nanoparticle dispersions were measured as the aforementioned methods.

2.12. Fourier transform infrared spectrum (FTIR)

The chemical structures of Gli NPs, TP, Gli/TP NPs, Cur and Cur/Gli/TP NPs were analyzed using a Fourier transform spectrophotometer (Thermo Scientific, Waltham, MA, USA). The procedure was as follows: The dried spectral pure-grade KBr powder was uniformly mixed with a small number of samples to be analyzed in an agate mortar, and then the mixtures were pressed into tablets. Finally, the spectra scanned at 500–4000 cm^{-1} were recorded and a resolution of 4 cm^{-1}. The test temperature was maintained at 25 °C (Zhang et al., 2021).

2.13. In vitro digestion

According to a previous reported method, the bioaccessibility of Cur-Gli/TP NPs and Cur-Gli NPs prepared at three different pH conditions (4.0, 5.0 and 7.0) was measured in a static simulated gastrointestinal model (GIT) (Li et al., 2021). Firstly, the fresh nanoparticle dispersions (20 mL) were mixed with simulated gastric fluid (pepsin: 0.032 g, NaCl: 0.04 g, pH 1.2) of equal volume (Wei and Huang, 2019). Then, the resulting mixtures were adjusted to pH 1.2 and digested under 37.0 °C for 2 h. After gastric digestion, the solution was adjusted to pH 7.5 to inhibit the activity of pepsin. Subsequently, the incubation solution was added into simulated intestinal juice of equal volume ($CaCl_2$: 0.022 g, pig bile salt: 0.2 g, tris: 0.12 g, pancreatin: 0.064 g, pH 7.5) (Wei and Huang, 2019). The sample was adjusted back to pH 7.5 and incubated at a stirring speed of 100 rpm for 2 h in water bath of 37 °C. Finally, each sample was centrifuged at 10000 rpm for 10 min to extract the supernatant, and free Cur was measured by a UV-2355 spectrophotometer (UNICO (Shanghai) Instrument CO. Ltd). Cur-Gli NPs at pH 4.0, 5.0 and 7.0 were used as control samples. The bioaccessibility of Cur was calculated as follows:

$$Bioaccessibility(\%) = \frac{mass\ of\ Cur\ added\ before\ digestion - mass\ of\ free\ Cur}{mass\ of\ Cur\ added\ before\ digestion} \times 100\% \quad (3)$$

2.14. Statistical analysis

All measurements were obtained in at least triplicate. Origin 2019b software was employed to perform statistical analysis. Data were analyzed by one-way analysis of variance (ANOVA) procedure with Duncan's multiple comparison test using the SPSS 13.0 software and accepted at $p < 0.05$.

3. Results and discussion

3.1. Characteristics of Gli/TP NPs

3.1.1. Influence of mass ratios on the nanoparticles

Fig. S1 showed a schematic representation of the process of Gli/TP NPs and Cur-Gli/TP NPs. The particle size, PdI, zeta-potential and turbidity of Gli/TP NPs with different mass ratios of Gli to TP were depicted in Fig. 1. The particle size generally affects the physicochemical properties, storage stability, encapsulation efficiency and bioavailability of nanoparticles (Wang et al., 2020; Xin et al., 2020). In the absence of TP, the particle size of Gli NPs was 198 ± 2.4 nm at pH 5.0. The particle size increased after adding TP, which might be accounted for the negatively charged TP bound to surface of Gli NPs through some interaction forces (i.e., electrostatic interactions, hydrophobic interactions as well as hydrogen bond) between Gli and TP. As seen in Fig. 1A, when the mass ratios of Gli to TP were 2:1, 1:1 and 1:2, the particle sizes of Gli/TP NPs were 332.7 ± 16.34 nm, 300.6 ± 3.89 nm and 585.2 ± 24.66 nm, respectively. When the mass ratios of Gli to TP were 2:1 and 1:1, respectively, sufficient TP was adsorbed onto the surface of Gli to form nanoparticles with excellent stability. As the mass ratio of Gli to TP continuously increased (Gli/TP mass ratio of 1:2), the particle size of Gli/TP NPs increased, which might be accounted for the aggregation of nanoparticles caused by excessive free TP. The dispersity of nanoparticles is usually characterized by polydispersity index (PdI), which reflects the particle size distribution of nanoparticles (Ding et al., 2021). The lower the PdI value is, the more uniform the nanoparticle size is. Generally, PdI <0.3 indicates that the dispersity of samples is relatively ideal (Meng et al., 2021). The PdI of Gli/TP NPs was <0.2, suggesting that all nanoparticles with diverse Gli/TP mass ratios (2:1, 1:1, 1:2) had homogeneous dispersion state (Fig. 1A).

The zeta-potential is often employed to characterize the stability of nanoparticles. Nanoparticles possessing higher absolute value of zeta-potential are relatively more stable. Since the formation of Gli/TP NPs might be largely affected by electrostatic interaction, the zeta-potential of these nanoparticles was studied (Wei et al., 2019a,b,c,d). As presented in Fig. 1B, when the mass ratios of Gli to TP were 2:1 and 1:1, the zeta-potentials of Gli/TP NPs were −24.8 ± 0.4 mV and −25.3 ± 0.55 mV, respectively, and these nanoparticles had slightly higher stability than that of the nanoparticles prepared at Gli/TP mass ratio of 1:2 with −21.8 ± 0.2 mV. The phenomenon might be explained by the fact that more negative charges were conducive to increasing the repulsion

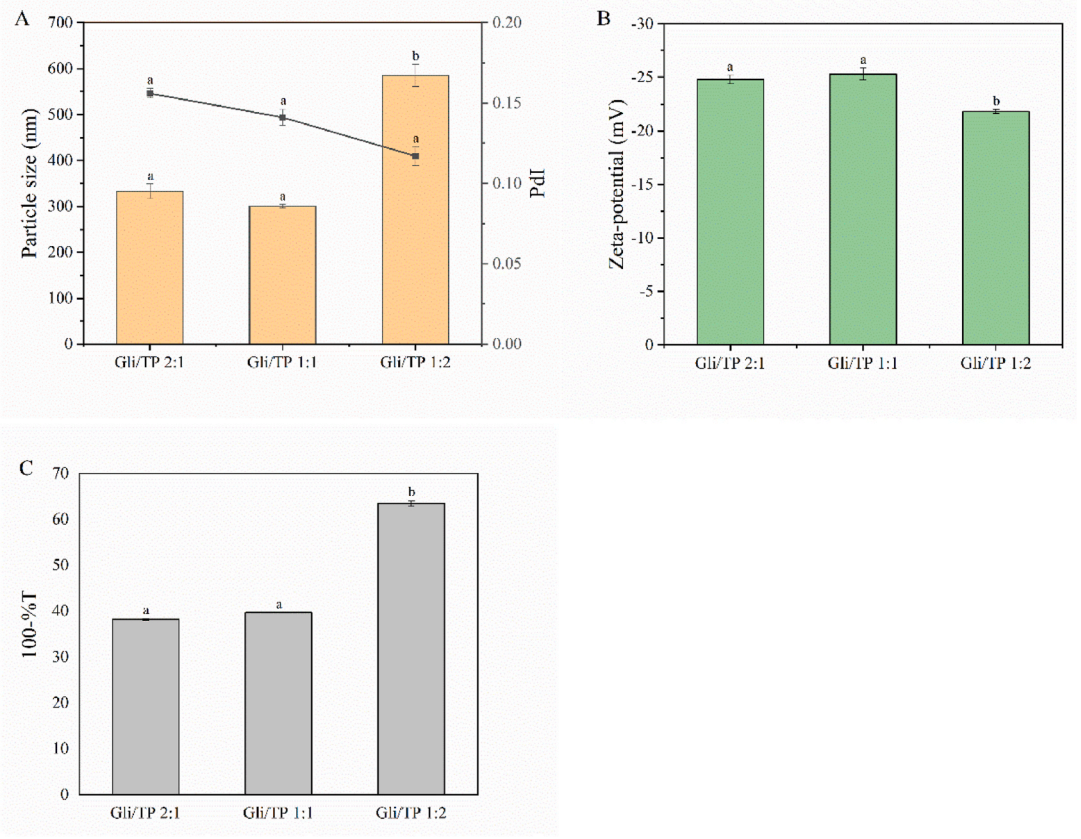

Fig. 1. Particle size and PdI (A), zeta-potential (B) and turbidity (C) of gliadin/tremella polysaccharide nanoparticle (Gli/TP NPs) with mass ratios of Gli to TP at 2:1, 1:1 and 1:2.

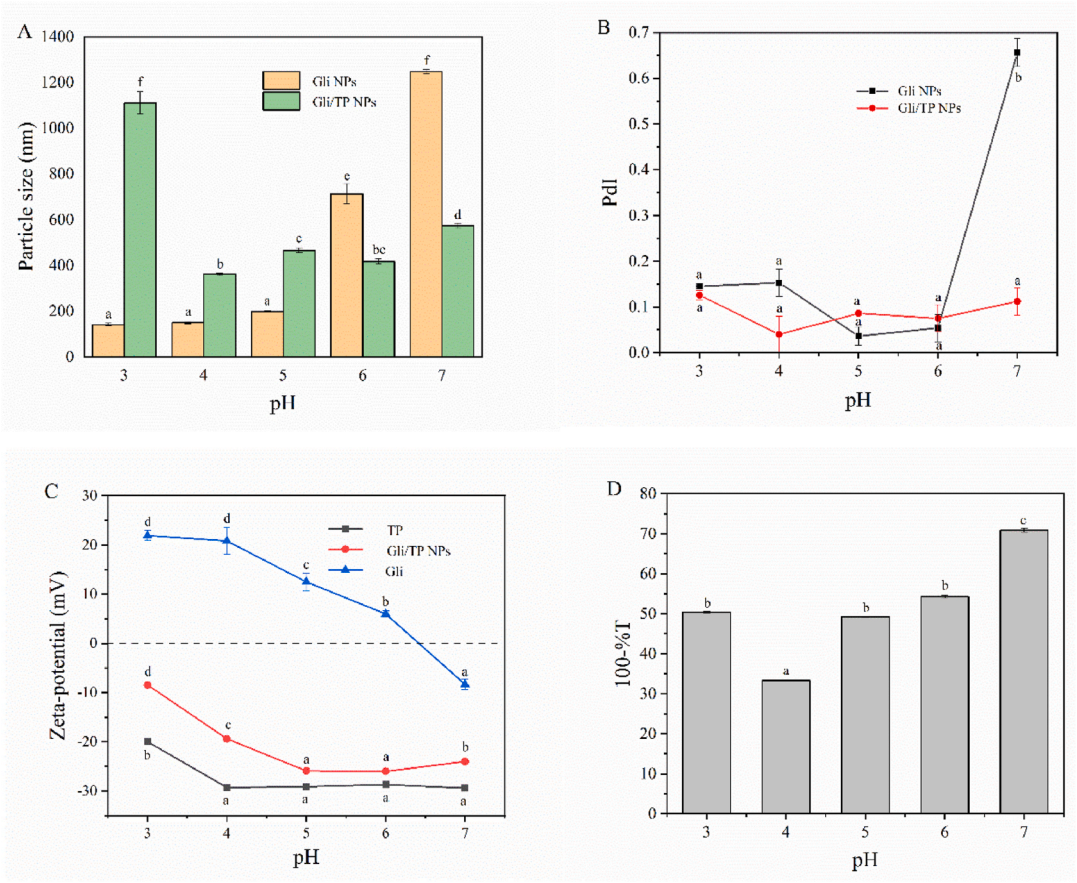

Fig. 2. Particle size (A), PdI (B), zeta-potential (C) and turbidity (D) of Gli/TP NPs (Gli/TP mass ratio 1:1) at pH 3.0, 4.0, 5.0, 6,0 and 7.0.

between nanoparticles, and thus resulting in lower collision frequency. Turbidity is usually considered as a function of particle size and concentration, the change of turbidity can be used to analyze the phase behavior of separation or binding in Gli/TP NPs (Wei et al., 2019). As depicted in Fig. 1C, the turbidity of Gli/TP NPs 2:1 and Gli/TP NPs 1:1 was significantly lower than that of Gli/TP NPs 1:2. The reason for the increase of turbidity of Gli/TP NPs 1:2 was that excessive TP was adsorbed on Gli nanoparticles allowing Gli/TP NPs to carry less negative charge. As the electrostatic repulsion decreased, the nanoparticles may approach closer, leading to the formation of unstable flocculation (Su et al., 2021). Considering the stability of nanoparticles, in the subsequent studies, Gli/TP NPs with a mass ratio of 1:1 were used to encapsulate Cur.

3.1.2. Influence of pH values on the nanoparticles

The particle size, PdI, zeta-potential and turbidity of Gli/TP NPs with different pH values were revealed in Fig. 2. As shown in Fig. 2A, Gli NPs had superior stability at pH 3.0–5.0 with the particle size of less than 200 nm. However, the particle size of the sample increased at pH 6.0, indicating that nanoparticles started to aggregate under this pH value. This might be accounted for that Gli NPs had less charge at this pH value that was close to isoelectric point (6.5) of Gli (Peng et al., 2018). By contrast, the particle size of Gli/TP NPs was larger at pH 3.0 (1110 ± 48.2 nm) and smaller at pH 4.0–7.0. The PdI of Gli NPs and Gli/TP NPs was shown in Fig. 2B. The PdI of Gli NPs at pH 7.0 was close to 0.6, which further confirmed result in Fig. 2A, indicating that Gli NPs was already aggregated at pH 7.0. However, the PdI of Gli/TP NPs at pH 3.0–7.0 was below 0.2, demonstrating that TP could improve the anti-agglomeration ability of nanoparticles and make nanoparticles uniformly dispersed.

The repulsion provided by the surface charge of nanoparticles plays an important role in maintaining the stability of nanoparticles. In Fig. 2C, the zeta-potential of Gli NPs prepared by anti-solvent method changed from positive charge to negative charge as pH values increased. The zeta-potential of +21.9 ± 1.05 mV to +5.97 ± 0.66 mV at pH 3.0–6.0 could provide sufficient repulsion force between the Gli NPs to maintain stability. However, the charge of Gli decreased when the pH value was close to its isoelectric point (6.5), which promoted the aggregation of the nanoparticles. The zeta-potential of TP was negative at pH 3.0–7.0 and its absolute value increased with the increase of pH values. By adding TP to Gli NPs, Gli/TP NPs had a high absolute potential at pH 4.0–6.0, indicating that the addition of TP greatly improved the electrostatic interaction between nanoparticles and thus contributed to producing stable nanoparticles. At pH 7.0, hydrogen bonding and hydrophobic interaction might be main interaction between Gli and TP, and they were also beneficial to maintaining stability between nanoparticles (D. Wang et al., 2019; Zhang et al., 2020; Wu et al., 2018).

The turbidity of Gli/TP NPs was presented in Fig. 2D. The turbidity of Gli NPs was lower and had no obvious change at pH 3.0–7.0. When Gli NPs and TP were mixed together, the strong interaction led to the appearance of solution immediately changed from transparency to turbidity. Among them, the Gli/TP NPs solution at pH 4.0–5.0 was relatively clear. At pH 3.0, the turbidity of Gli/TP NPs was high, which was consistent with the result of particle size in Fig. 2A, indicating that the stability of Gli/TP NPs at this pH value was inferior. Although the electrostatic interaction between Gli and TP was slight at pH 7.0, hydrogen bonding and hydrophobic interaction could also promote the stability of the nanoparticles at this pH value (Su et al., 2021). Therefore, the optimal pH of Gli/TP NPs were 4.0 and 5.0. We should also be aware that the formation mechanism of Gli/TP NPs at pH 7.0 (exceeding the isoelectric point of Gli) was different from that at pH 4.0 and 5.0. Thus, Gli/TP NPs with various pH values (4.0, 5.0 and 7.0) were chosen for

Table 1
Characterization of Cur-Gli/TP NPs with different Gli to Cur mass ratios.

Gli to Cur mass ratios	Sample pH	Particle size (nm)	PdI	Zeta-potential (mV)	Encapsulation efficiency (%)
4:1	4.0	359.9 ± 8.55^{a}	0.14 ± 0.1^{ab}	−19.2 ± 0.7^{de}	88.4 ± 0.45^{a}
	5.0	348.6 ± 10.32^{a}	0.094 ± 0.02^{a}	−24.9 ± 0.42^{b}	88.5 ± 0.27^{a}
	7.0	830 ± 31.39^{b}	0.291 ± 0.01^{c}	−22.6 ± 0.21^{c}	82.6 ± 0.8^{a}
2:1	4.0	394.1 ± 4.59^{a}	0.068 ± 0.05^{a}	−20.1 ± 0.35^{d}	90.5 ± 0.6^{b}
	5.0	390 ± 1.76^{a}	0.079 ± 0.03^{a}	−26.8 ± 1.41^{a}	90.6 ± 0.52^{b}
	7.0	452.8 ± 10.6^{a}	0.166 ± 0.02^{b}	−25.2 ± 0.98^{b}	83.9 ± 0.4^{a}
1:1	4.0	1440 ± 246.07^{c}	0.615 ± 0.1^{d}	−19.1 ± 0.56^{e}	92.8 ± 0.33^{b}
	5.0	2166 ± 108.18^{d}	0.586 ± 0.02^{d}	−25.5 ± 0.63^{b}	93.8 ± 0.21^{b}
	7.0	4055 ± 382.5^{e}	0.321 ± 0.03^{c}	−19.5 ± 0.63^{de}	95.8 ± 0.4^{c}

following studies.

3.2. Characteristics and encapsulation efficiency (EE) of Cur-Gli/TP NPs

The overall effect of different pH values and mass ratios of Gli to Cur on the particle size, PdI, zeta-potential and encapsulation efficiency of Cur-Gli NPs were summarized in Table S1. The particle sizes of Cur-Gli NPs with various Gli/Cur mass ratios (4:1, 2:1 and 1:1) at pH 4.0, 5.0 and 7.0 were about 200 nm, which suggested that these nanoparticles were relatively stable. After adding TP, the particle size of nanoparticles became larger, and Cur-Gli/TP NPs at different pH values and Gli/Cur mass ratios had diverse particle sizes (Table 1). Cur-Gli/TP NPs 4:1 and Cur-Gli/TP NPs 2:1 at pH 4.0 and 5.0 had a relatively smaller particle size and higher negative charge, and yet these nanoparticles possessed larger particle size at pH 7.0 due to the same positive charge of Gli and TP facilitating aggregation between nanoparticles (Chen et al., 2021). Moreover, the particle size of Cur-Gli/TP NPs 1:1 was over 1000 nm, which showed that these nanoparticles were unstable due to the over-saturation of Cur.

As for the EE of Cur, it could be seen that Cur-Gli NPs 2:1 at pH 5.0 had the best EE (58.2 ± 0.42%) in all Cur-Gli NPs with different mass ratios of Gli to Cur. Although the EE of Cur in Cur-Gli NPs increased with

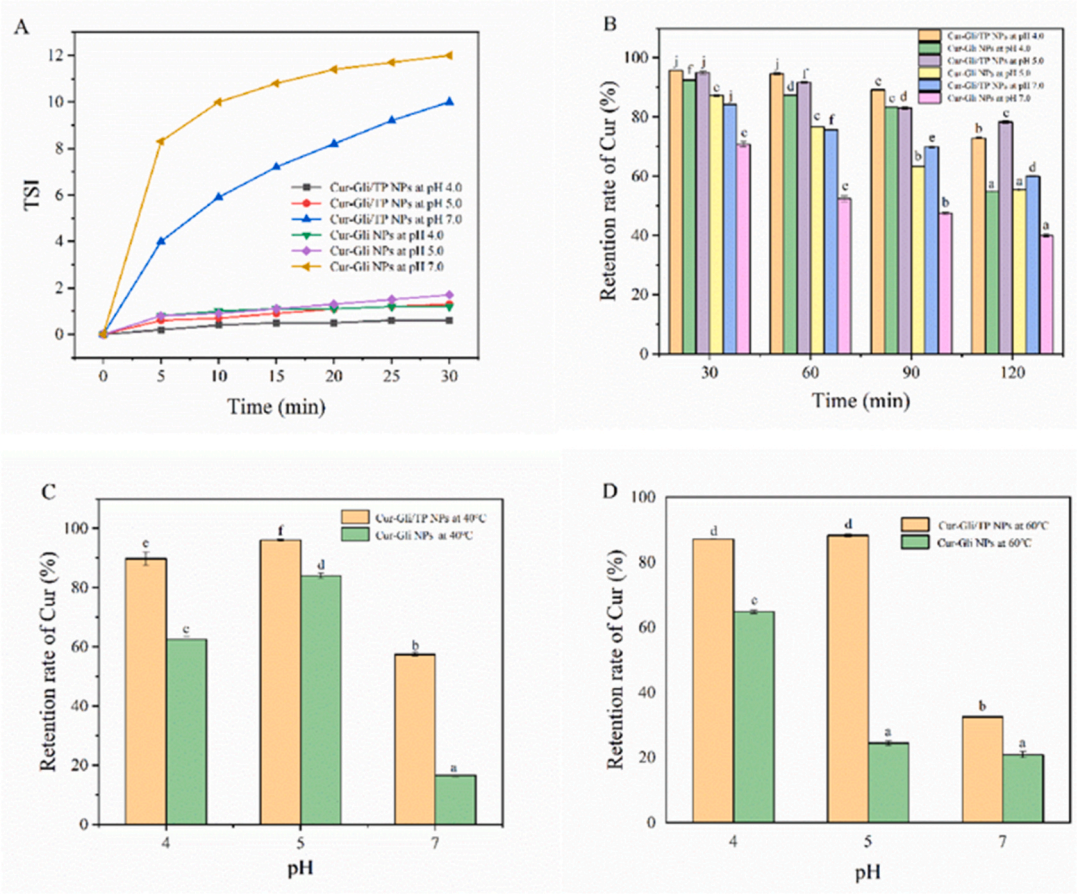

Fig. 3. (A)TSI profile of Cur-Gli/TP NPs and Cur-Gli NPs (Gli/Cur mass ratio 2:1) at pH 4.0, 5.0 and 7.0.(B)Retention rate (%) of curcumin in Cur-Gli/TP NPs and Cur-Gli NPs after UV light irradiation. (C) Retention rate (%) of curcumin in Cur-Gli/TP NPs and Cur-Gli NPs after thermal treatment at 40 °C for 30 min. (D) Retention rate (%) of curcumin in Cur-Gli/TP NPs and Cur-Gli NPs after thermal treatment at 60 °C for 30 min.

the increase of the mass ratio of Gli to Cur, the overall improvement effect was not very obvious, and the EE remained at a relatively low level. However, by adding TP, the EE of Cur-Gli/TP NPs was significantly higher than that of Cur-Gli NPs, which could be attributed to that TP formed a thick layer around the nanoparticles increasing the steric and electrostatic repulsion between the nanoparticles and suppressing the Cur release (Li et al., 2021). Moreover, the Cur-Gli/TP NPs had enhanced EE as the Gli to Cur mass ratios increased. Among them, when the mass ratios of Gli to Cur was 1:1, the EE of the Cur-Gli/TP NPs reached about 92.8 ± 0.33%, 93.8 ± 0.21% and 95.8 ± 0.4% at pH 4.0, 5.0 and 7.0, respectively, much higher than Cur-Gli NPs. However, the above characterization results have shown that Cur-Gli/TP NPs 1:1 cannot be used for industrial production due to their lower absolute zeta-potential values and too large particle size. Therefore, after comprehensive consideration, the Cur-Gli/TP NPs with mass ratio of Gli to Cur 2:1 were selected for follow-up studies. Similarly, in the previous study, Su and co-workers prepared gliadin/sodium alginate nanoparticles using anti-solvent method and applied these nanoparticles to encapsulate Cur. However, currently prepared Cur-Gli/TP NPs significantly had the higher EE (90.5%) of Cur than that of gliadin/sodium alginate nanoparticles (61.29%) (Su et al., 2021), which showed that TP played a relatively more important role in improving the EE of Cur.

3.3. Evaluation of stability of Cu-Gli/TP NPs

For a detailed characterization of application potential of new Cur-Gli/TP NPs, the stability of nanoparticles is crucial. The stability of the nanoparticles may be affected by several parameters such as pH values, UV light and heat, as the change of these conditions possibly leads to interactions facilitating the formation of sediment or flocculate between nanoparticles.

3.3.1. Physical stability

At room temperature (25 °C), the influence of different pH values on the physical stability of Cur-Gli NPs and Cur-Gli/TP NPs was evaluated by Turbiscan Lab Expert® (Fig. 3A). Each sample was measured for 30 min to obtain the TSI profiles of these nanoparticles at pH 4.0, 5.0 and 7.0. The results showed that the kinetic values of Cur-Gli NPs and Cur-Gli/TP NPs at pH 4.0 and 5.0 only varied slightly, which confirmed that there were no sediment and flocculation occurring in these samples and they had excellent physical stability. Meanwhile, compared with Cur-Gli NPs, the addition of TP did not lead to any significant difference in TSI of Cur-Gli/TP NPs (Cosco et al., 2019; Gagliardi et al., 2021). On the contrary, the TSI profiles of Cur-Gli NPs and Cur-Gli/TP NPs increased significantly at pH 7.0, which indicated that pH proximity to the isoelectric point of Gli (6.5) might promote the structural instability of these nanoparticles and produce precipitation (Voci et al., 2021).

3.3.2. Photostability

Poor photostability is one of the disadvantages of Cur, limiting its commercial applications. The effect of UV light on the stability of Cur at pH 4.0, 5.0 and 7.0 was exhibited in Fig. 3B. At pH 4.0, the retention rate of Cur in Cur-Gli/TP NPs after UV irradiation for 0.5, 1, 1.5 and 2 h was not much different from that of pH 5.0. However, at pH 7.0, the retention rate of Cur in nanoparticles was 20% lower than that of at pH 4.0 and 5.0, indicating the protective effects of Cur-Gli/TP NPs on Cur were not ideal enough at pH 7.0 compared with that at pH 4.0 and 5.0 under the condition of being exposed to UV light. Furthermore, compared with Cur-Gli NPs without TP, the photostability of all the Cur-Gli/TP NPs was superior. This suggested that the formation of TP layers provided better UV light resistance. Moreover, the higher turbidity of the nanoparticles was, the stronger the light scattering capability of the solution was, and thus the photostability of the Cur was better (Meng et al., 2021; Qiu et al., 2017).

3.3.3. Thermal stability

Heat is one of the main factors inducing the degradation of Cur. Therefore, it is necessary to investigate the effect of thermal treatment on Cur-Gli/TP NPs at pH 4.0, 5.0 and 7.0. The impact of heat treatment (40 °C and 60 °C) on stability of Cur in Cur-Gli/TP NPs and Cur-Gli NPs were evaluated for 30 min. As shown in Fig. 3C, when the Cur-loaded nanoparticle dispersions were heated at 40 °C for 30 min and at pH 4.0, 5.0 and 7.0, the retention rates of Cur in Cur-Gli/TP NPs were 89.8% ± 2.34%, 96.1% ± 0.36% and 57.3% ± 0.55%, respectively. While the retention rates of Cur in Cur-Gli NPs were 62.6% ± 0.77%, 84.1% ± 0.83% and 16.6% ± 0.49%, respectively. By adding TP, the retention rate of the nanoparticles increased by at least 20%. The results showed that the presence of TP layer had a superior ability to enhance thermal stability of Cur (Meng et al., 2021; Zheng et al., 2021). When the Cur-loaded nanoparticle dispersions were heated at 60 °C for 30 min (Fig. 3D), the retention rate of Cur in all nanoparticles displayed the same trend as that heated at 40 °C (Wu et al., 2018). Compared with Cur-Gli NPs, the retention rate of Cur in Cur-Gli/TP NPs increased by more than 20%, while that in Cur-Gli/lecithin NPs increased by less than 15% at 60 °C for 30 min (Yang et al., 2018). This indicated that TP had excellent ability to improve thermal stability of Cur, regardless of temperature.

3.4. Re-dispersibility

For commercial applications, powdered nanoparticles are more convenient to be transported, stored and sold than nanoparticles existing in liquid. Re-dispersibility is one of the important features for the nanoparticles dispersions that are frozen dried into powder products (Yuan et al., 2021). Therefore, the re-dispersibility of Cur-Gli/TP NPs and Cur-Gli NPs was evaluated. The particle size of re-dispersed Cur-Gli

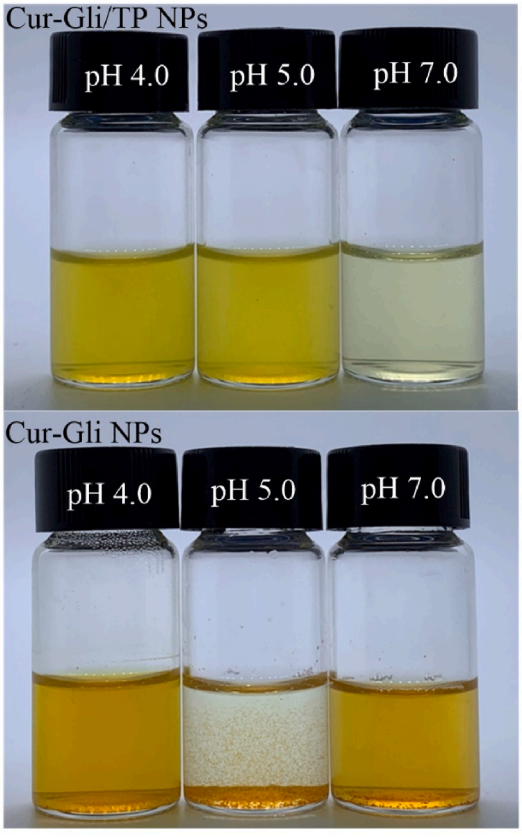

Fig. 4. Visual appearance on the samples of re-dispersed Cur-Gli/TP NPs and Cur-Gli NPs at pH 4.0, 5.0 and 7.0. The mass ratio of Gli to Cur was 2:1.

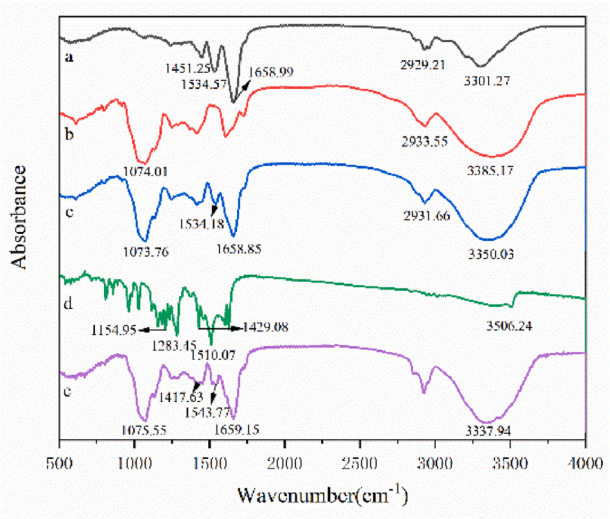

Fig. 5. FTIR spectra of Gli NPs (a), TP (b), Gli/TP NPs(c), Cur (d) and Cur-Gli/TP NPs (e).

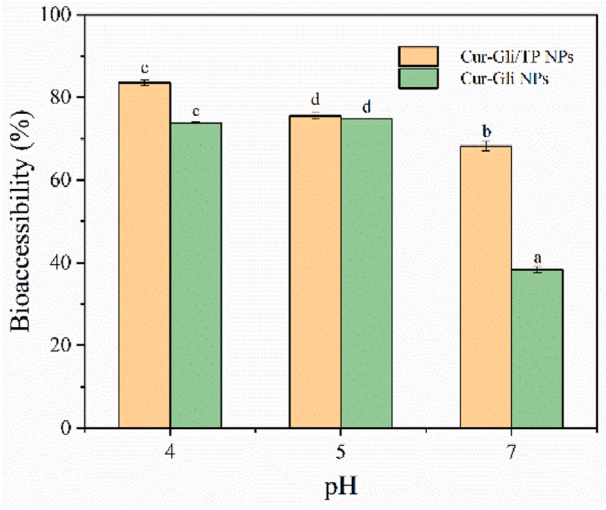

Fig. 6. Bioaccessibility of Cur in Cur-Gli/TP NPs and Cur-Gli NPs at pH 4.0, 5.0 and 7.0. The mass ratio of Gli to Cur was 2:1.

NPs and Cur-Gli/TP NPs were shown in Table S2. The redispersed Cur-Gli-NPs and Cur-Gli/TP NPs had larger particle size at pH 4.0, 5.0, and 7.0 than in fresh samples, probably due to aggregation of particles during drying process. The result was similar to the particle size of re-dispersed curcumin-loaded gliadin-rhamnolipid composite nanoparticles. The appearances of the re-dispersed nanoparticles were shown in Fig. 4. The re-dispersed Cur-Gli/TP NPs at pH 4.0, 5.0 and 7.0 did not show any aggregation and precipitation. However, the re-dispersed Cur-Gli NPs (without TP) at pH 4.0, 5.0 and 7.0 were very unstable and precipitated. In particular, the re-dispersed nanoparticles were almost insoluble at pH 5.0 and 7.0. This might be due to the hydrophilic group of TP increased the water binding capacity of Cur-Gli/TP NPs, while Gli possessed a large amount of hydrophobic amino acids, preventing the Cur-Gli NPs from being re-dispersed. The results indicated the Cur-Gli/TP NPs possessed more excellent re-dispersibility than Cur-Gli NPs (Chen et al., 2021; Yuan et al., 2021).

3.5. FTIR analysis

FTIR is a method that can quickly and effectively identify chemical molecules in a polymer matrix (Xue et al., 2021). Hence, we used it to analyze Gli NPs, TP, Gli/TP NPs, Cur and Cur-Gli/TP NPs to study the possible interactions among the nanoparticles (Fig. 5). The O–H stretching vibration (3100–3500 cm^{-1}) of Gli/TP NPs and Cur-Gli/TP NPs were different with Gli, TP and Cur. These differences imply that hydrogen bonding was generated among Gli, TP and Cur. Both Gli and Cur are hydrophobic substances; thus, there are hydrophobic interactions between them (Qu et al., 2021). Moreover, the characteristic peaks of Gli were 1658.99 $cm^{-1}$and 1534.57 cm^{-1}, which represented amide I (C = O stretching) and amide II (N = H bending). After adding TP and Cur, the peaks of amide I in the spectrum of Gli/TP NPs and Cur-Gli/TP NPs were respectively shifted to 1658.85 $cm^{-1}$and 1659.15 cm^{-1}, and those of amide II were respectively shifted to 1543.18 $cm^{-1}$and 1543.77 cm^{-1}. This finding indicated that electrostatic interaction existed among Gli, TP and Cur. The characteristic peak of TP was at 1074.01 cm^{-1}, which appeared in the spectra of Gli/TP NPs (1073.76 cm^{-1}) and Cur-Gli/TP NPs (1075.55 cm^{-1}) (Jiang et al., 2021).

For native Cur, the characteristic peaks of Cur represented the stretching vibration of the aromatic rings (1429.08 cm^{-1}), part of "keto" (1283.45 cm^{-1}), and the inter-ring chain (1154.95 cm^{-1}). However, these peaks were not observed in the Cur-Gli/TP NPs because the binding of Cur with Gli/TP NPs nanoparticles limited the stretching and bending of the chemical bonds in Cur, indicating that Cur was successfully encapsulated in the Gli/TP NPs (Zhang et al., 2021).

3.6. Bioaccessibility of Cur

Gli/TP NPs were further utilized as Cur-loaded delivery vehicles, and the bioaccessibility of Cur was studied to evaluate the delivery efficiency of Gli/TP NPs on Cur. The bioaccessibility of Cur was studied using *in vitro* digestive models. The bioaccessibility of Cur-Gli/TP NPs and Cur-Gli NPs in the simulated gastrointestinal tract was illustrated in Fig. 6. Under simulated gastrointestinal conditions, the bioaccessibility of Cur in Cur-Gli/TP NPs and Cur-Gli NPs decreased as pH increased, indicating that the weaker interaction between Gli and TP led to the lower Cur bioaccessibility. After release of 120 min in the small intestine stimulation fluid, the bioaccessibility of Cur in Cur-Gli/TP NPs at pH 4.0, 5.0 and 7.0 were 83.5% ± 0.7%, 75.7% ± 0.77% and 68.2% ± 1.13%, respectively, whereas the bioaccessibility which was less than the former of Cur in Cur-Gli NPs at pH 4.0, 5.0 and 7.0 were 73.8% ± 0.14%, 74.8% ± 0.07% and 38.3% ± 0.77%, respectively. In addition, the bioaccessibility of Cur in all nanoparticles was higher at pH 4.0 and 5.0 than that at pH 7.0 (He et al., 2021; Elbaz et al., 2021). The bioaccessibility of Cur in Cur-Gli/TP NPs was 75.5%, which was higher than that of gliadin-chitosan nanoparticles (25%) (Zeng et al., 2019) and gliadin-sodium alginate nanoparticles (55%) (Su et al., 2021). Since Cur-Gli/TP NPs can improve the bioaccessibility of Cur, we can conclude that Cur-Gli/TP NP is a suitable platform for delivering hydrophobic compounds of nutritional interest.

4. Conclusion

In conclusion, novel curcumin-loaded gliadin/tremella polysaccharide nanoparticles (Cur-Gli/TP NPs) were successfully prepared by anti-solvent method. It was found that different mass ratios of Gli to TP and pH values had great effects on the formation of Gli/TP NPs. Through a series of characterizations on the prepared nanoparticles, it has been found that the nanoparticles possessed excellent stability at Gli to TP mass ratio of 1:1 and pH 4.0–7.0. Subsequently, Cur-Gli/TP NPs were prepared and studied at different pH values, and hydrogen bonding, electrostatic interactions as well as hydrophobic interactions participated in the formation of Cur-Gli/TP NPs. Cur-Gli/TP NPs showed significantly higher encapsulation efficiency (90.6% ± 0.52%) of Cur, as compared with Cur-Gli NPs (58.2% ± 0.42%). Moreover, TP exhibited a positive effect on improving the stability and re-dispersibility of Cur-Gli/TP NPs. The physics, UV light and thermal stability of Cur-Gli/TP

NPs were better than that of those Cur-Gli NPs (without TP). This may be due to the presence of TP that makes the Cur-Gli NPs structure more compact. *In vitro* digestion study revealed that Gli/TP NPs improved the bioaccessibility of Cur. In conclusion, TP possesses strong potential in improving the EE, stability and bioaccessibility of Cur in Gli NPs.

CRediT authorship contribution statement

Xiaomin Zhang: Investigation, Software, Data curation, Writing – original draft. **Zihao Wei:** Conceptualization, Methodology, Resources, Software, Writing – review & editing, Project administration, Funding acquisition, Supervision. **Xin Wang:** Writing – review & editing. **Yuming Wang:** Writing – review & editing. **Qingjuan Tang:** Writing – review & editing. **Qingrong Huang:** Writing – review & editing. **Changhu Xue:** Writing – review & editing.

Declaration of competing interest

The authors declare that they have no known competing financial interests or personal relationships that could have appeared to influence the work reported in this paper.

Acknowledgments

This work was supported by the start-up fund from Ocean University of China (grant No. 862001013134). This work was also funded by the National Key R&D Program of China (grant No. 2018YFC0311201). We thank Dr. Xiao Song in Ocean University of China for providing the polysaccharide samples.

Appendix A. Supplementary data

Supplementary data to this article can be found online at https://doi.org/10.1016/j.crfs.2022.01.019.

References

Chen, S., Ma, Y., Dai, L., Liao, W., Zhang, L., Liu, J., Gao, Y., 2021. Fabrication, characterization, stability and re-dispersibility of curcumin-loaded gliadin-rhamnolipid composite nanoparticles using pH-driven method. Food Hydrocolloids 118, 106758.

Chen, X., Zhang, T., Wu, Y., Gong, P., Li, H., 2021. Foxtail millet prolamin as an effective encapsulant deliver curcumin by fabricating caseinate stabilized composite nanoparticles. Food Chem. 36, 130764.

Cosco, D., Mare, R., Paolino, D., Salvatici, M., Cilurzo, F., Fresta, M., 2019. Sclareol-loaded hyaluronan-coated PLGA nanoparticles: physico-chemical properties and *in vitro* anticancer features. Int. J. Biol. Macromol. 132, 550–557.

Dhingra, D., Bisht, M., Bhawna, B., Pandey, S., 2021. Enhanced solubility and improved stability of curcumin in novel water-in-deep eutectic solvent microemulsions. J. Mol. Liq. 100, 117037.

Ding, Z., Mo, M., Zhang, K., Bi, Y., Kong, F., 2021. Preparation, characterization and biological activity of proanthocyanidin-chitosan nanoparticles. Int. J. Biol. Macromol. 188, 45–51.

Elbaz, N., Tatham, L., Owen, A., Rannard, S., McDonald, T., 2021. Redispersible nanosuspensions as a plausible oral delivery system for curcumin. Food Hydrocolloids 121, 107005.

Feng, S., Sun, Y., Wang, D., Sun, P., Shao, P., 2020. Effect of adjusting pH and chondroitin sulfate on the formation of curcumin-zein nanoparticles: synthesis, characterization and morphology. Carbohydr. Polym. 250, 116970.

Gagliardi, A., Paolino, D., Costa, N., Fresta, M., Cosco, D., 2021. Zein- vs PLGA-based nanoparticles containing rutin: a comparative investigation. Mater. Sci. Eng. C 118, 111538.

Ge, X., Huang, W., Xu, X., Lei, P., Sun, D., Xu, H., Li, S., 2020. Production, structure, and bioactivity of polysaccharide isolated from Tremella fuciformis XY. Int. J. Biol. Macromol. 148, 173–181.

He, J., Zhu, J., Yin, S., Yang, X., 2021. Bioaccessibility and intracellular antioxidant activity of phloretin embodied by gliadin/sodium carboxymethyl cellulose nanoparticles. Food Hydrocolloids 122, 107076.

Jiang, F., Yang, L., Wang, S., Ying, X., Ling, J., Ouyang, X., 2021. Fabrication and characterization of zein-alginate oligosaccharide complex nanoparticles as delivery vehicles of curcumin. J. Mol. Liq. 342, 116937.

Li, Z., Lin, Q., McClements, D., Fu, Y., Xie, H., Li, T., Chen, G., 2021. Curcumin-loaded core-shell biopolymer nanoparticles produced by the pH-driven method : physicochemical and release properties. Food Chem. 355, 129686.

Meng, R., Wu, Z., Xie, Q., Cheng, J., Zhang, B., 2021. Preparation and characterization of zein/carboxymethyl dextrin nanoparticles to encapsulate curcumin: physicochemical stability, antioxidant activity and controlled release properties. Food Chem. 340, 127893.

Niu, B., Feng, S., Xuan, S., Shao, P., 2021. Moisture and caking resistant Tremella fuciformis polysaccharides microcapsules with hypoglycemic activity. Food Res. Int. 146, 110420.

Peng, D., Jin, W., Tang, C., Lu, Y., Wang, W., Li, J., Li, B., 2018. Foaming and surface properties of gliadin nanoparticles: influence of pH and heating temperature. Food Hydrocolloids 77, 107–116.

Qiu, C., Wang, B., Wang, Y., Teng, Y., 2017. Effects of colloidal complexes formation between resveratrol and deamidated gliadin on the bioaccessibility and lipid oxidative stability. Food Hydrocolloids 69, 466–472.

Qu, B., Xue, J., Luo, Y., 2021. Self-assembled caseinate-laponite® nanocomposites for curcumin delivery. Food Chem. 363, 130338.

Su, C., Huang, Y., Chen, Q., Li, M., Wang, H., Li, G., 2021. A novel complex coacervate formed by gliadin and sodium alginate : relationship to encapsulation and controlled release properties. Lebensm. Wiss. Technol. 139, 110591.

Voci, S., Gagliardi, A., Salvatici, M., Fresta, M., Cosco, D., 2021. Development of polyoxyethylene (2) oleyl ether-gliadin nanoparticles: characterization and *in vitro* cytotoxicity. Eur. J. Pharmaceut. Sci. 162, 105849.

Wang, D., Wang, D., Yan, T., Jiang, W., Han, X., Yan, J., Guo, Y., 2019. Nanostructures assembly and the property of polysaccharide extracted from Tremella Fuciformis fruiting body. Int. J. Biol. Macromol. 137, 751–760.

Wang, S., Lu, Y., Ouyang, X., Ling, J., 2020. Fabrication of soy protein isolate/cellulose nanocrystal composite nanoparticles for curcumin delivery. Int. J. Biol. Macromol. 165, 1468–1474.

Wang, Y., Yan, W., Li, R., Jia, X., Cheng, Y., 2019. Impact of deamidation on gliadin-based nanoparticle formation and curcumin encapsulation. J. Food Eng. 260, 30–39.

Wei, Z., Zhu, J., Cheng, Y., Huang, Q., 2019a. Ovotransferrin fibril–stabilized Pickering emulsions improve protection and bioaccessibility of curcumin. Food Res. Int. 125, 108602.

Wei, Z., Cheng, Y., Huang, Q., 2019b. Heteroprotein complex formation of ovotransferrin and lysozyme: fabrication of food-grade particles to stabilize Pickering emulsions. Food Hydrocolloids 96, 190–200.

Wei, Z., Cheng, Y., Zhu, J., Huang, Q., 2019c. Genipin-crosslinked ovotransferrin particle-stabilized Pickering emulsions as delivery vehicles for hesperidin. Food Hydrocolloids 94, 561–573.

Wei, Z., Huang, Q., 2019. Developing organogel-based Pickering emulsions with improved freeze-thaw stability and hesperidin bioaccessibility. Food Hydrocolloids 93, 68–77.

Wei, Z., Zhu, P., Huang, Q., 2019d. Investigation of ovotransferrin conformation and its complexation with sugar beet pectin. Food Hydrocolloids 87, 448–458.

Wu, W., Kong, X., Zhang, C., Hua, Y., Chen, Y., 2018. Improving the stability of wheat gliadin nanoparticles – effect of gum Arabic addition. Food Hydrocolloids 80, 78–87.

Wu, W., Kong, X., Zhang, C., Hua, Y., Chen, Y., Li, X., 2020. Fabrication and characterization of resveratrol-loaded gliadin nanoparticles stabilized by gum Arabic and chitosan hydrochloride. Lebensm. Wiss. Technol. 129, 109532.

Wu, Y., Wei, Z., Zhang, F., Linhardt, R., Sun, P., Zhang, A., 2019. Structure, bioactivities and applications of the polysaccharides from Tremella fuciformis mushroom: a review. Int. J. Biol. Macromol. 121, 1005–1010.

Xiao, H., Li, H., Wen, Y., Jiang, D., Zhu, S., He, X., Xiong, Q., Gao, J., Hou, S., Huang, S., He, L., Liang, J., 2021. Tremella fuciformis polysaccharides ameliorated ulcerative colitis via inhibiting inflammation and enhancing intestinal epithelial barrier function. Int. J. Biol. Macromol. 180, 633–642.

Xin, S., Xiao, L., Dong, X., Li, X., Wang, Y., Hu, X., Sameen, D., Qin, W., Zhu, B., 2020. Preparation of chitosan/curcumin nanoparticles based zein and potato starch composite films for Schizothorax prenati fillet preservation. Int. J. Biol. Macromol. 164, 211–221.

Xu, X., Chen, A., Ge, X., Li, S., Zhang, T., Xu, H., 2020. Chain conformation and physicochemical properties of polysaccharide (glucuronoxylomannan) from fruit bodies of Tremella fuciformis. Carbohydr. Polym. 245, 116354.

Xue, J., Li, Z., Duan, H., He, J., Luo, Y., 2021. Chemically modified phytoglycogen: physicochemical characterizations and applications to encapsulate curcumin. Colloids Surf. B Biointerfaces 205, 111829.

Yang, S., Dai, L., Sun, C., Gao, Y., 2018. Characterization of curcumin loaded gliadin-lecithin composite nanoparticles fabricated by antisolvent precipitation in different blending sequences. Food Hydrocolloids 85, 185–194.

Yang, S., Liu, L., Chen, H., Wei, Y., Dai, L., Liu, J., Yuan, F., Mao, L., Li, Z., Chen, F., Gao, Y., 2021. Impact of different crosslinking agents on functional properties of curcumin-loaded gliadin-chitosan composite nanoparticles. Food Hydrocolloids 112, 106258.

Yu, J., Wang, Q., Zhang, H., Qin, X., Chen, H., Corke, H., Hu, Z., Liu, G., 2021. Increased stability of curcumin-loaded Pickering emulsions based on glycated proteins and chitooligosaccharides for functional food application. Lebensm. Wiss. Technol. 148, 111742.

Yuan, D., Zhou, F., Shen, P., Zhang, Y., Lin, L., Zhao, M., 2021. Self-assembled soy protein nanoparticles by partial enzymatic hydrolysis for pH-driven encapsulation and delivery of hydrophobic cargo curcumin. Food Hydrocolloids 120, 106759.

Yuan, Y., Xiao, J., Zhang, P., Ma, M., Wang, D., Xu, Y., 2021. Development of pH-driven zein/tea saponin composite nanoparticles for encapsulation and oral delivery of curcumin. Food Chem. 364, 130401.

Zeng, Q., Li, M., Li, Z., Zhang, J., Wang, Q., Feng, S., Su, D., He, S., Yuan, Y., 2019. Formation of gliadin-chitosan soluble complexes and coacervates through pH-induced: relationship to encapsulation and controlled release properties. Lebensm. Wiss. Technol. 105, 79–86.

Zhan, X., Dai, L., Zhang, L., Gao, Y., 2020. Entrapment of curcumin in whey protein isolate and zein composite nanoparticles using pH-driven method. Food Hydrocolloids 106, 105839.

Zhang, H., Jiang, L., Tong, M., Lu, Y., Ouyang, X., Ling, J., 2021. Encapsulation of curcumin using fucoidan stabilized zein nanoparticles: preparation, characterization, and *in vitro* release performance. J. Mol. Liq. 329, 115586.

Zhang, X., Liang, H., Li, J., Wei, X., Li, B., 2020. Improving the emulsifying property of gliadin nanoparticles as stabilizer of Pickering emulsions: modification with sodium carboxymethyl cellulose. Food Hydrocolloids 107, 105936.

Zhao, H., Li, Y., 2020. A novel pH/temperature-responsive hydrogel based on tremella polysaccharide and poly(N-isopropylacrylamide). Colloids Surf. A Physicochem. Eng. Asp. 586, 124270.

Zheng, W., Chen, Z., Yang, Y., Yang, R., Yang, T., Lai, P., Chen, T., Qiu, S., Wang, S., Liao, L., 2021. Improved stabilization of coix seed oil in a nanocage-coating framework based on gliadin–carboxymethyl chitosan-Ca^{2+}. Carbohydr. Polym. 257, 117557.